

REPORT TITLE: Point Buchon Ocean Bottom Seismometer Project

SIGNATORIES

PREPARED BY: Marcia McLaren DATE: 06/29/2014

Marcia McLaren PG&E
Printed Name Organization

VERIFIED BY: Megan Stanton DATE: 06/29/2014

Megan Stanton PG&E
Printed Name Organization

APPROVED BY: Richard Klimczak DATE: 09/10/2014

Richard Klimczak PG&E - Geosciences
Printed Name Organization

RECORD OF REVISIONS

Rev. No.	Reason for Revision	Revision Date
0	Initial Report. This work is defined and tracked in SAPN 50631543	06/29/2014

TABLE OF CONTENTS

	Page
Signatories Page	1
Record of Revisions	2
Lists of Tables, Figures, Appendices, and Attachments.....	4
Abbreviations and Acronyms	7
1.0 INTRODUCTION	9
1.1 Objectives	9
1.2 Background.....	10
2.0 PRE-DEPLOYMENT ACTIVITIES	12
2.1 Analysis by Waldhauser for Optimum OBS Locations	12
2.2 Lease and Permits	13
2.3 System Layout and Instrumentation	14
3.0 DEPLOYMENT	16
4.0 RESULTS.....	19
4.1 Noise Survey.....	19
4.1.1 Deployment and Recovery.....	19
4.1.2 Data Analysis.....	20
4.2 Analysis of Earthquakes Recorded by the OBS Units	21
4.2.1 Analytical Tests	22
4.2.2 Earthquake Relocation Results.....	22
4.2.3 Earthquake Focal Mechanism Results.....	23
5.0 SOFTWARE	29
6.0 CONCLUSIONS	30
7.0 REFERENCES	31

LISTS OF TABLES, FIGURES, APPENDICES, AND ATTACHMENTS

Tables

- Table 4-1 Analysis of Earthquakes Recorded by OBS
Table 4-2 Results of Event Tests

Figures

- Figure 1-1 Central Coast Region Seismic Networks
Figure 1-2 OBS and On-Land Seismic Stations with Seismicity
- Figure 2-1 Sensitivity Analyses for Optimum OBS Station Locations
Figure 2-2 Sensitivity Analyses: Location and Error Results Using Synthetic Event Locations
Figure 2-3 Seafloor Habitats with Installed OBS and Cable Locations, Marine Protected Area and Original Planned OBS and Cable Locations Shown in Faded Colors
Figure 2-4 OBS Instrumentation
- Figure 3-1 OBS Deployment
Figure 3-2 (a) Vertical Seafloor Profile and (b) Water Depth and Habitat Type for As-Laid Cable Route from OBS-4 to DCP.P Shoreline Intake
- Figure 4-1 Noise Survey: OBS Location Relative to the Waverider Buoy
Figure 4-2 Noise Survey: Temporary OBS Units
Figure 4-3 Noise Survey: Short-Period Noise Recorded on Temp-2
Figure 4-4 Noise Survey: Long-Period Noise Recorded on Temp-1 and Temp-2
Figure 4-5 Noise Survey: DPG Recording and Spectrogram
Figure 4-6 Noise Survey: Temp-1 vs. Temp-2 Recordings Example of Artificial Noise
Figure 4-7 Earthquake Location Study Using OBS Recorded Data
Figure 4-8 Comparison of the USGS and PG&E CCSN Velocity Models
Figure 4-9 OBS Recordings for the M 2.35 Earthquake on 28 Nov 2013
Figure 4-10 Focal Mechanisms for the M 2.35 Earthquake on 28 Nov 2013—Original NCSN Catalog Data with OBS-4 Data (USGS Velocity Model)

- Figure 4-11 Focal Mechanisms for the M 2.35 Earthquake on 28 Nov 2013—Original NCSN Catalog Data with OBS-4 Data (PG&E Velocity Model)
- Figure 4-12 Focal Mechanism for the M 2.35 Earthquake on 28 Nov 2013—Original NCSN Catalog Data with No OBS Data (PG&E Velocity Model)
- Figure 4-13 Focal Mechanisms for the M 2.35 Earthquake on 28 Nov 2013—Original NCSN Catalog Data with All OBS Data (USGS Velocity Model)
- Figure 4-14 OBS Recordings for the M 0.81 Earthquake on 08 Feb 2014
- Figure 4-15 Focal Mechanisms for the M 0.81 Earthquake on 08 Feb 2014—Original NCSN Catalog Data with OBS-1 and -4 Data (USGS Velocity Model)
- Figure 4-16 Focal Mechanisms for the M 0.81 Earthquake on 08 Feb 2014—Original NCSN Catalog Data with OBS-1 and -4 Data, (PG&E Velocity Model)
- Figure 4-17 Focal Mechanisms for the M 0.81 Earthquake on 08 Feb 2014—Original NCSN Catalog Data with No OBS Data (PG&E Velocity Model)
- Figure 4-18 OBS Recordings for the M 1.24 Earthquake on 11 Feb 2014
- Figure 4-19 Focal Mechanisms for the M 1.24 Earthquake on 11 Feb 2014—Original NCSN Catalog Data with All OBS Data (USGS Velocity Model)
- Figure 4-20 Focal Mechanism for the M 1.24 Earthquake on 11 Feb 2014—Original NCSN Catalog Data with All OBS Data (PG&E Velocity Model)
- Figure 4-21 Focal Mechanisms for the M 1.24 Earthquake on 11 Feb 2014—Original NCSN Catalog Data with No OBS Data (PG&E Velocity Model)
- Figure 4-22 Focal Mechanisms for the M 1.24 Earthquake on 11 Feb 2014—Original NCSN Catalog Data with All OBS Data and Added PG&E S-Wave Picks (USGS Velocity Model)
- Figure 4-23 OBS-4 Recording for the M 0.88 Earthquake on 01 Apr 2014
- Figure 4-24 Focal Mechanisms for the M 0.88 Earthquake on 01 Apr 2014—Original NCSN USGS Catalog Data with OBS-4 Data (USGS Velocity Model)
- Figure 4-25 Focal Mechanisms for the M 0.88 Earthquake on 01 Apr 2014—Original NCSN Catalog Data with OBS-4 Data, (PG&E Velocity Model)
- Figure 4-26 Focal Mechanisms for the M 0.88 Earthquake on 01 Apr 2014—Original NCSN USGS Catalog Data with No OBS Data (PG&E Velocity Model)

Appendices

- Appendix A Sensitivity Study (Dr. Felix Waldhauser)
- Appendix B Calibrations, Hydrostatic Test Report, and Technical Manual
- Appendix C Acceptance Test Plans and Final Judgements
- Appendix D PG&E Site Acceptance Test Results
- Appendix E As-Laid ROV Survey
- Appendix F Post-Deployment Nearshore Diver Survey
- Appendix G Noise Survey

Attachments

- Attachment 1 Report Verification Summary

ABBREVIATIONS AND ACRONYMS

ANSS	Advanced National Seismic System
ATP	acceptance test plan
CCC	California Coastal Commission
CCSN	Central Coast Seismic Network
CDP	Coastal Development Permit
CEQA	California Environmental Quality Act
CISN	California Integrated Seismic Network
CSLC	California State Lands Commission
DCPP	Diablo Canyon Power Plant
DPG	differential pressure gauge
FAT	factory acceptance test
Guralp	Guralp Systems Ltd.
Hz	hertz
km	kilometer(s)
LTSP	Long Term Seismic Program
m	meter(s)
M	magnitude
MND	Mitigated Negative Declaration
MPA	Marine Protected Area
NCSN	Northern California Seismic Network
NRC	U.S. Nuclear Regulatory Commission
OADC	Optimal Anisotropic Dynamic Clustering
OBS	ocean-bottom seismometer
PDT	pre-deployment acceptance test
PG&E	Pacific Gas and Electric Company
Pre-FAT	pre-factory acceptance test
RFP	request for proposal
ROV	remotely operated vehicle
s	second(s)
SAPN	SAP [software] notification

SAT	site acceptance test
USACE	U.S. Army Corps of Engineers
USGS	U.S. Geological Survey
UTC	Coordinated Universal Time

1.0 INTRODUCTION

As part of Pacific Gas and Electric Company's (PG&E's) assessment of seismic safety at the Diablo Canyon Power Plant (DCPP),¹ four ocean-bottom seismometers were installed as a cabled system (herein referred to as the "OBS system") to collect earthquake data in the nearshore waters off Point Buchon in San Luis Obispo County, California. The Point Buchon Ocean-Bottom Seismometer (OBS) Project (herein referred to as the "OBS Project") involved planning and preparation, deployment of the OBS instruments, and analysis of recorded data. The OBS system is expected to remain in operation for up to 10 years.

The planning and deployment of the OBS system were not performed under a nuclear quality assurance (NQA) program. However, this technical report has been written and reviewed by a qualified Independent Technical Reviewer in accordance with PG&E Geosciences procedures TQ1.GE1 and CF3.GE2 (see Attachment 1). In addition, this report serves to document the instrument deployment and provide evidence that the instruments and cable were formally accepted through documented calibrations and factory, site, and final, signed accepted tests. Completion of this report is tracked under SAPN 50631543-1.

This technical report describes the OBS system and the various activities that completing the deployment entailed. The rest of this section presents the objectives of the OBS Project and background information, including a detailed description of Dr. Jeanne Hardebeck's initial work to image the Shoreline seismicity lineament. Section 2.0 describes the pre-deployment activities, including obtaining a state lease and state and federal permits, and analysis to find the optimum locations for OBS placement. Section 3.0 describes the deployment process, including the factory, site, and final acceptance tests, and the post-deployment, as-laid, diver surveys and remotely operated vehicle (ROV) surveys. Section 4.0 describes the results of the data collection, including the results of a noise survey to study the sources of noise that would be expected in a shallow-water environment, and an analysis of four earthquakes recorded by the OBS units. Section 5.0 presents the conclusions related to the deployment process and the data analyses. Section 6.0 lists the literature sources referred to in this report.

1.1 Objectives

The primary objectives of the OBS Project are as follows:

- Use the OBS system to record earthquakes in real time that occur within the region offshore of the DCPP and integrate the data recorded on the OBS system with data recorded on the onshore PG&E and U.S. Geological Survey (USGS) seismic networks (Figure 1-1). A further objective is to transmit the OBS data and

¹ This work is being done by PG&E to comply with the California Energy Commission (CEC) recommendation, stated in the CEC's November 2008 report titled *An Assessment of California's Nuclear Power Plants: AB 1632 Report*, that PG&E use three-dimensional (3D) seismic-reflection mapping and other advanced geophysical techniques to explore fault zones near the DCPP.

the on-land PG&E data to PG&E's Central Coast Seismic Network (CCSN) Earthworm computer system in San Francisco, California, and then stream the data to the USGS in Menlo Park, California, for public use.

- Provide full waveform data for small-magnitude ($M < 3$) earthquakes and on-scale acceleration recordings of large-magnitude ($M > 3$) earthquakes.
- Reduce the inherent uncertainties in offshore earthquake locations and subsequent focal mechanisms. These uncertainties exist in the region offshore from the DCP.P simply because the earthquakes occur outside the on-land networks and do not have adequate azimuthal coverage.

The ultimate goal of the OBS system is to use improved locations and focal mechanisms of offshore earthquakes to constrain the downdip geometry and sense of slip of the Hosgri fault zone and Shoreline fault and provide evidence as to whether the faults are connected.

1.2 Background

In November 2008, PG&E informed the U.S. Nuclear Regulatory Commission (NRC) that preliminary results from the Diablo Canyon Power Plant (DCPP) Long Term Seismic Program (LTSP) update showed that an alignment of microseismicity existed sub-parallel to the coastline, indicating the possible presence of a previously unidentified fault approximately 1 kilometer (km) offshore of the DCP.P (PG&E, 2011). This seismicity lineament was imaged by Dr. Jeanne Hardebeck using an earthquake relocation program called tomoDD (Zhang and Thurber, 2003), a double-difference program that jointly inverts for locations and velocity structure by using both absolute and differential arrival time data. Double-difference is a method of relocating earthquakes relative to one another. The imaging using the tomoDD program resulted in both improved resolution of structures outlined by the seismicity patterns and improved accuracy of locations. Hardebeck subsequently published her results in the *Bulletin of the Seismological Society of America* (Hardebeck, 2010).

Figure 1-2 shows the Hardebeck (2010) published locations, together with locations that she added through December 2013 (J. Hardebeck, pers. comm., 2014). The additional locations include one event (M 1.2, at 2.6 km depth) along the Shoreline fault approximately 4 km southeast from the DCP.P; another event (M 1.6, at 13.2 km depth) within the diffuse seismicity where the Shoreline fault approaches the Hosgri fault zone; and about 10 other small ($M < 1.7$) earthquakes scattered along the Hosgri fault zone from approximately latitude 35.33N to 35.05N. Hardebeck's database also includes a location for the 28 November 2013 earthquake, which is analyzed in Section 4.2 and referred to as Event 1. The location of this event is marked on Figure 4-7.

Hardebeck (2010) presented earthquake relocations and focal mechanisms within a regional study area that was centered on the offshore Hosgri fault zone and Shoreline fault. She used tomoDD to compute the relocations and HASH software (Hardebeck and Shearer, 2002) to compute focal mechanisms. HASH uses first-motion P-wave data and ray tracing through a 3D seismic-velocity model in the program. Hardebeck's results

show seismicity alignments along the Hosgri fault zone and Shoreline fault offshore from the DCP.P, with the more westerly trending Shoreline fault approaching the Hosgri fault zone (Hardebeck, 2010). Seismicity associated with the Hosgri fault zone extends nearly vertical to about 12 km depth. The earthquakes that comprise the Shoreline seismicity lineament nearest the DCP.P extend to about 10 km depth, while the earthquakes in the region where the Shoreline fault approaches the Hosgri fault zone extend to 12–15 km depth.

Focal mechanisms along both the Hosgri fault zone and Shoreline fault showed predominantly right-lateral strike-slip motion along northwest- and west-northwest-trending faults, respectively. However, the focal mechanisms along the portion of the Hosgri fault zone near Point Buchon and along the Shoreline fault were “D” quality, which is the lowest quality. Hardebeck’s (2010) tectonic model shows the Shoreline fault connected to the Hosgri fault zone, as interpreted from connecting composites of these D-quality focal mechanisms along the Shoreline fault and Hosgri fault zone. Hardebeck concluded that future studies were needed to constrain the geometry and possible connection of the Shoreline fault with the Hosgri fault zone.

Hardebeck continued her study of the Hosgri fault zone and Shoreline fault geometries at depth and their possible connection. To identify the planar fault geometries that fit all the input locations of approximately 100 newly relocated earthquakes to within their location uncertainty (Hardebeck, 2013), she used an algorithm developed by Ouillon et al. (2008) called Optimal Anisotropic Dynamic Clustering (OADC; Hardebeck, 2013). She then compared the resulting fault plane orientations to the fault planes from composite focal mechanisms of events along the Shoreline fault and Hosgri fault zone, with an emphasis on composites below 8 km depth along the shoreline fault.

The results using the OADC method showed the Shoreline fault as a continuous vertical fault that connects with the Hosgri fault zone beneath approximately 8 km depth, and the Hosgri fault zone as either dipping steeply to the east and under the Shoreline fault or dipping vertically with some other structure underlying the Shoreline fault. The composite focal mechanisms generally agree with right slip on the Hosgri fault zone and Shoreline fault planes created using the OADC method. Similar to Hardebeck (2010), the composite mechanisms were needed because all the new mechanisms were D-quality single-event mechanisms. The need to determine high-quality offshore earthquake locations and focal mechanisms through better azimuthal station coverage was a primary motivation for deploying an OBS system.

2.0 PRE-DEPLOYMENT ACTIVITIES

As part of the pre-deployment activities before the OBS could be installed, a vendor was chosen and a system design and instrumentation were sought; in addition, a lease and permits from various state and federal agencies were obtained, including several environmental permits. The optimal system design had to consider both the project's scientific goals and environmental impacts to marine life on the ocean floor.

Planning and system design consisted of choosing a vendor and designing the layout of each OBS station. The layout had to be completed before we could start the lease and permitting process (see Section 2.2). Choosing a vendor for this project entailed soliciting bids through a Request for Proposal (RFP). To create the RFP, we needed to communicate to the prospective vendors the approximate locations where the OBS units would be installed and the various state and federal agency requirements. To specify a layout for potential bidders to consider and to prepare for creating the various documents required by the permitting agencies, we contracted Dr. Felix Waldhauser of the Lamont Doherty Earth Observatory to provide a sensitivity analysis of the optimum locations. The analysis would use a synthetic data set of offshore events for a maximum of four OBS units and would target the area where the Shoreline fault approached the Hosgri fault zone, in the region of diffuse seismicity (Hardebeck, 2014; Figure 1-2). Section 2.1 describes the analysis that was performed to choose an optimum configuration for the OBS system. Section 2.2 summarizes the lease and permit process.

2.1 Analysis by Waldhauser for Optimum OBS Locations

Dr. Waldhauser's method was to demonstrate the ability of a given OBS configuration with existing on-land seismic stations to accurately locate offshore seismicity. The various iterations that Dr. Waldhauser performed are listed in Appendix A. To start, he set up a grid of offshore synthetic sources (open circles on Figure 2-1) and designed an initial configuration of the four OBS units. He then iteratively moved the OBS units, within certain constraints (e.g. not on faults), until they optimized the station criteria that he set to monitor the target area (the intersection between the Hosgri fault zone and Shoreline fault).

The red and yellow sources shown on both maps of Figure 2-1 are the sources with the optimal criteria for the OBS configuration shown. Red indicates that the sources have the following network criteria:

- At least one station within 5 km (to constrain shallow events).
- At least three stations within 10 km (to best constrain events down to seismogenic depth).
- A maximum azimuthal gap less than 180 degrees (to constrain the epicenter).

Yellow sources have more stringent network criteria, as follows:

- At least one station within 3 km.
- At least three stations within 10 km.
- A maximum azimuthal station gap less than 110 degrees.

Both the red and yellow sources are constrained to 12 km depth; the yellow sources are better constrained at shallow depths.

Maps were created for several sets of OBS configurations and for maximum distances of 20 and 55 km to simulate small and larger earthquakes (Figure 2-1, top and bottom views, respectively). The OBS configuration shown on Figure 2-1 is not optimal, but it does show that the target is reliably covered. This was the approximate configuration that was used in the RFP. As discussed in Section 2.2, the final proposed configuration was modified to comply with requirements by state and federal agencies and to avoid certain seafloor habitats (e.g., rocky areas).

In addition, synthetic travel times for P and S waves were computed using the grid of synthetic sources (open circles) and the velocity model of McLaren and Savage (2001) to obtain the network parameters for each source. The USGS earthquake location computer software HYPOINVERSE-2000 (Klein, 2002) was used to invert the synthetic travel times for hypocenter locations. After testing the solutions for sensitivity to various noise levels, he added normally distributed noise to the “perfect” synthetic locations, with standard deviations of 0.05 s for stations out to 55 km, and 0.1 s for stations out to 20 km. The synthetic hypocenter locations and corresponding errors are shown on the top and bottom views of Figure 2-2, for stations recording out to 20 km and 55 km, respectively. As expected, the top view shows larger location errors than those on the bottom view, particularly for events along the Hosgri fault zone, as the top view represents fewer stations contributing to the locations and larger azimuthal gaps.

The results of this sensitivity analysis, as seen in both the distribution of the better network criteria (red and yellow circles), shown on Figure 2-1, and the size of the location errors, shown on Figure 2-2, indicate that we can expect reliable locations of events with the target area for small and larger events.

2.2 Lease and Permits

Our choice of deployment area within state tidelands created some leasing and permitting difficulties. One key siting consideration was to avoid areas of active commercial bottom trawling; for this reason, we chose to stay within the state’s 3-nautical-mile boundary (Figure 2-3). Consequently, we had to traverse part of the state’s recently designated Marine Protected Area (MPA; blue polygon on Figure 2-3). However, within the MPA, we were restricted from entering the state marine reserve (easternmost blue polygon on Figure 2-3), except for the south corner, west of OBS-4. We were also required to stay within the sandy soft-sediment areas and avoid impacts to sensitive hard-bottom habitat. The mapped seafloor habitat shows that the rockiest areas are between the OBS-4 location and the shoreline.

For a deployment within the 3-nautical-mile boundary, we were required to obtain a lease from the California State Lands Commission (CSLC), as well as permits from the California Coastal Commission (CCC) and U.S. Army Corp of Engineers (USACE). For each agency we were required to submit a project description. Implicit in the requirements of all the agencies was consideration of the seafloor environment and avoidance of impacts to known sensitive habitat.

The process to obtain the lease and permits involved the following steps:

1. A Mitigated Negative Declaration (MND) was prepared by the CSLC, as the lead agency under the California Environmental Quality Act (CEQA), to analyze and disclose the environmental effects associated with PG&E's OBS Project (CSLC, 2012). PG&E supported CSLC's preparation of the MND by providing a draft of the MND to the CSLC in March 2012. The draft MND contained a full description of the project, including instrumentation, deployment specifics (e.g., boat specifications, locations for placement of the cable and instruments, time of year of deployment), and acknowledgment of environmental issues (e.g., whale migrations, presence of seals and sea lion rookeries and haulouts, and ocean-bottom flora and fauna that could be affected by the instruments on the ocean floor). During a CSLC hearing, the MND was certified, the project approved, and the Offshore Lease Agreement issued. The lease would not be finalized and signed, and the payment decided, until after the deployment was completed and documented in a report from PG&E summarizing a seafloor ROV survey of the cable route and OBS installation locations, and a diver survey of the cable route in the DCP.P intake (Appendices E and F).
2. The CCC required application for a Coastal Development Permit (CDP) before the OBS systems could be installed. PG&E submitted a permit application package that included data on the site characterization, as well as information on the OBS systems. A staff report with a recommendation for approval was completed by the CCC staff. The CDP was approved during a public hearing before the Commission. As part of the CCC approval process, PG&E made a contribution to a fund managed by the University of California, Davis that supports the SeaDoc Society, a nonprofit organization that works to protect marine wildlife and their habitat; the group strives to keep the California ocean floor free of debris.
3. Once the CCC approved the CDP, the USACE completed its process to issue a Nationwide Permit (NWP-5) for the installation and operation of the scientific instrumentation.
4. Other required permits included a Scientific Collecting Permit from the California Department of Fish and Wildlife for placement of the OBS systems within the state MPA. A notification document was also submitted to the State Water Resources Control Board, Central Coast Region, in support of the USACE approval.

2.3 System Layout and Instrumentation

Guralp Systems Ltd. (Guralp), based in Reading, England, was chosen as the vendor to provide the cable and instrumentation and perform the deployment. The OBS system layout consisted of four long-term OBS units, or stations, placed in shallow water no more than 3 nautical miles from the coast. The stations were daisy-chained to a single multistranded cable, which provided shore power to each station (Figure 2-4a) and transmitted data to a shore-based facility within the DCP.P (Figure 2-3). Two temporary

OBS units were to be installed for approximately two weeks at two different locations to provide data for analysis of the various noise sources (see Section 4.1). Figure 2-3 shows the original planned cable layout and long-term and temporary OBS locations as red lines and blue and yellow diamonds, respectively. Details of the results of the deployments, including the final cable and OBS locations, are described in Section 3.0.

The instrumentation for each long-term OBS station consists of a three-component broadband seismometer (Guralp CMG-3T), a three-component accelerometer (Guralp CMG-5T), and a 24-bit digitizer/data logger (Figure 2-4b). The combination of accelerometer and velocity is consistent with the USGS Advanced National Seismic System (ANSS) model for seismographic stations and the majority of onshore seismic stations of PG&E's CCSN. The equipment is housed in a titanium casing (Figure 2-4c), which is covered by a concrete cap (dome) weighing more than 1 metric ton (Figure 2-4d). The dome secures and protects the equipment. The OBS station closest to shore is equipped with a differential pressure gauge (DPG) attached to the dome. The temporary OBS units were equipped with Guralp CMG-40T seismometers.

The signals from each long-term OBS station will be digitized in situ and then transmitted via dedicated optical fiber inside the cable to a shore station at the DCP.P. From there, the data will be streamed in real time to PG&E's CCSN Earthworm computer system in San Francisco and, ultimately, exported to the USGS's Earthworm system in Menlo Park for integration with the Northern California Seismic Network (NCSN). The NCSN is one of five networks that make up the California Integrated Seismic Network (CISN). CISN is one of eight networks that make up the ANSS.

3.0 DEPLOYMENT

Once the agency permits were signed in June 2013, we were allowed to begin the deployment process. The first deployment activity involved agreement between Guralp and PG&E on an acceptance test plan (ATP). The ATP consisted of four levels of tests to be completed at different stages of the project:

1. Pre-factory acceptance test (Pre-FAT).
2. Factory acceptance test (FAT).
3. Pre-ocean-bottom deployment acceptance test (PDT).
4. Site acceptance test (SAT).

At each stage, acceptance tests verified that the previous tests had been completed and approved. The pre-FAT and FAT were conducted in June 2013 at the Guralp facility in England. The PDT was conducted at the Morro Bay Power Plant in Morro Bay, California in July 2013 after the OBS system was assembled. The SAT was conducted at the recording station at the DCP.P intake, at the completion of the deployment in November 2013.

The pre-FAT verified that all model numbers and serial numbers of all components were listed on the receipt, that calibration sheets were available for all instruments to be tested, and that all major subsystems of the OBS system were connected and ready to be tested. The FAT consisted of checking all OBS components and cables, including calibrations of the seismic instruments and pressure tests of the titanium boxes. After the FAT was completed, the cable and instruments, including the 1-ton concrete caps (Figure 2-4d), were shipped from England in early July to a staging area at the Morro Bay Power Plant.

The PDT consisted of connecting the four OBS units (Figure 2-3c) to the cables (Figure 2-3a) and checking the system to ensure that the units could receive power from a power source and could transmit data back to a laptop computer (the same laptop that was to be used in the recording station at the intake). The SAT conducted performance and functionality checks of the complete OBS system.

The ATP was signed on 21 June 2013 by a representative from Guralp and a representative from PG&E's seismic instrumentation contractor, M. Cullen Instruments of Petaluma, California. The FAT was completed and signed on the same day. The PDT was completed and signed on 13 July 2013, and the SAT was completed and signed on 24 November 2013. The technical manual for the OBS system and the results from the instrument calibrations and pressure tests are documented in Appendix B. The ATP, which describes the various tests and sign-offs (called "Judgements"), is provided in Appendix C. The SAT results are documented in Appendix D.

The M/V *Surveyor*, an approximately 30 m (100-foot) steel-hulled boat, was used to deploy the long-term and temporary OBS units and cable. Figure 3-1a shows an OBS unit with cables connected and ready for deployment. Figure 3-1b shows the OBS and cable being deployed off the stern of the *Surveyor*. The titanium box sits up inside the dome, with the broadband sensor's "feet" extending below the dome.

Lowering each unit into the water at the designated location was a critical part of the deployment. It was important to lower the units into the water as gently and as level as possible (i.e., not at an angle) so that they would be placed flat on the seafloor. Our goal was to aim for sand so that the weight of the domes would help couple the seismometer's sensor "feet" evenly to the seafloor. This was a challenge when there were windy or swell conditions because it was difficult for the crew to lower the unit into the water evenly and for the *Surveyor* to hold its position.

Another critical part of the deployment was laying the cable in the DCP.P intake bay. Figure 3-1c shows a schematic of the cable route into the intake and ultimately to the onshore recording center. The cable entered the DCP.P facility through a PVC conduit that extends into the marine waters of the DCP.P intake. The *Surveyor* had to lay the cable into the deeper part of the intake and then pass the cable on to the divers who would lay the last few meters of cable from the boat's location to the conduit and thread the cable through the conduit. A shore crew then pulled the cable from the conduit, threaded it into the shore facility, and attached it to the recording center. To prevent the *Surveyor* from damaging the intake structure, a tugboat was commissioned to stay between them (Figure 3-1d). For safety reasons, the *Surveyor* was required to cut its motor while the boat crew handed off the cable to the divers. The *Surveyor* was given special permission to temporarily anchor in the intake during this hand-off process.

Figure 2-4 shows where the cables and long-term and temporary OBS units were ultimately laid (red lines and blue and yellow diamonds, respectively). OBS units 1, 2, and 3, and the cable linking them were deployed in sandy areas, along with the two temporary units, Temp-1 and Temp-2. The junction box and nearby cable between OBS units 3 and 4 were deployed in rockier areas, along with the cable between OBS-4 and the DCP.P intake to the conduit. The final OBS locations and portion of the cable lay from OBS-1 to within about 200 yards of the mouth of the intake were documented by the as-laid ROV survey (Appendix E). The portion of the cable lay from the end of the ROV survey, near the mouth of the intake, to the conduit was documented by the nearshore diver survey (Appendix F).

Figure 3-2 is a detailed view of the route between OBS-4 and the intake to the conduit at the shoreline, as obtained by the ROV survey and the nearshore diver survey (Appendices E and F). OBS-4 sits on soft sediments, while the cable extends across both soft and hard sediments. Video from the post-laid ROV survey confirms that the OBS-4 unit was deployed flat on the seafloor and that although the cable does traverse some rocky areas, the cable at the time of the ROV survey was not at risk of being damaged by the rocks (Appendix E). However, because of the potential for strong currents and high swell in this shallow nearshore region, particularly near the mouth of the intake, the cable could sustain damage in the future. We authorized the divers, at their suggestion after their nearshore survey (Appendix F), to add extra armoring (tubing) to the cable to mitigate potential damage to the cable from the mouth of the intake to the conduit. Future ROV surveys from the intake to OBS-4 are being considered to monitor potential damage to the cable along that part of the cable route.

Initial installation was completed between 20 July and 27 July 2013; all four OBS units and approximately 11.5 miles (18.5 km) of cable were deployed. However, because the cable broke between OBS stations 2 and 3, and salt water leaked into the junction boxes between OBS stations 3 and 4, only OBS-4 was in operation at the end of the July installation. Final adjustments to the system were completed between 6 November and 24 November 2013, with all stations in operation. The final SAT (Appendix D) was completed by Guralp, and the “Final Judgement” (Appendix C) was signed by PG&E and Guralp on 24 November 2013.

It should be noted that because weather caused delays in the schedule, it was decided in July to leave the two temporary units, Temp-1 and Temp-2, at their locations until the beginning of the final adjustment period in November, rather than taking the time to recover and redeploy the units to locations Temp-3 and Temp-4, as originally planned (Figure 2-4). Temp-1 and Temp-2 were recovered from their locations on 7 November 2013.

4.0 RESULTS

In this section we analyze the results obtained from data recorded on the temporary and long-term OBS instruments. Section 4.1 describes the noise survey conducted by Guralp using data from the two temporary OBS units. The survey captured a variety of noise sources and defined the most dominant noise. Section 4.2 presents an analysis of four small earthquakes recorded by the long-term OBS stations that were located nearby. Focal mechanisms are included in the analyses of the earthquakes.

4.1 Noise Survey

Because the long-term OBS units are installed in shallow water, at depths between 60 and 120 m, the wave action and swell at the sea surface affect the sensor recordings more strongly than if the OBS equipment were installed in deep water. To our knowledge, this is the shallowest known deployment off the California coast. Because the noise was expected to be highly variable, we decided to conduct a noise survey using broadband velocity sensors similar to the sensors used in the long-term OBS units.

Our original plan was to conduct the noise survey in stages, deploying the two temporary units at least a month before installing the long-term stations, and using the survey results to guide deployment of the long-term station locations. The two units would be deployed at the Temp-1 and Temp-2 locations for two weeks (faded yellow diamonds of Figure 2-4), then they would be recovered and redeployed for another two weeks at sites Temp-3 and Temp-4. However, our permit consultant believed it would be best to conduct the deployments concurrently, thereby minimizing the disruption to marine life, and to leave them in place during the three months between initial installation in July and final installation in November. Consequently, we modified our noise survey plan to study the various noise sources recorded on the temporary OBS units Temp-1 and Temp-2 and then compare those recordings to the DPG atop OBS-4 and to data from the DCP.P waverider buoy.

Figure 4-1 shows a map of the locations of the long-term and temporary OBS units and the waverider buoy. Temp-2 was deployed on 25 July 2013 at 70 m depth, and Temp-1 was deployed on 27 July 2013 at 106 m depth. Both units were recovered on 7 November 2013. Temp-2 was deployed for 106 days and Temp-1 was deployed for 104 days. However, the batteries did not last as long as the deployment; consequently, Temp-2 recorded for only 99 days and Temp-1 recorded for 96 days, with no data gaps in either unit. The noise survey performed by Guralp is discussed below. The full survey is provided in Appendix G.

4.1.1 *Deployment and Recovery*

Figure 4-2a shows the instruments in their pre-deployment configuration. Each OBS unit consists of a frame, two sealed glass spheres, the sensor package, anchor weights (concrete ballasts), and peripheral equipment. The glass spheres, which contain the batteries, digitizer, and data storage device, are protected by orange plastic covers. The

sensor package is mounted in the center, underneath the frame (Figure 4-2b). The sensor is housed in a smaller glass sphere, which in turn is contained in a stainless steel frame.

Deploying the units involved lowering each by winch and wire rope to the ocean bottom. To keep the units from drifting across the seafloor because of currents, chains were added to the base of the frame (Figure 4-2c). The concrete ballasts also helped stabilize the units during deployment.

Normally, at the time of recovery, an acoustic transponder releases the frame from the ballasts, leaving them on the seafloor. However, as stipulated in our lease and the Scientific Collecting Permit, we were not allowed to leave anything on the seafloor. Guralp modified the recovery process for each unit by connecting a line from the unit to a clump weight. A second line was attached to the clump weight with buoys and floaters at the ocean surface end to make the unit easier to find later. The winch was used to recover both the temporary units and the clump weight. Attaching the buoys to the second line worked for Temp-1; however, Temp-2 lost its buoys and floaters, and an ROV was needed to recover the weight and the unit (Figure 4-2d).

4.1.2 Data Analysis

Analyses of the short-period and long-period noise and artificial noise, and a comparison of DPG and waverider buoy data are given below. Spectrograms are used to visually represent the frequencies contained in the time series. In contrast to a spectrum or a power spectral density plot, the spectrogram shows how the amplitudes of the various noise sources vary over time. The hotter colors (yellow to red) represent the areas within the spectrum of highest intensity of noise. The spectrogram scale on the right shows the amplitudes in the frequency band. The Nyquist frequency is 100 Hz, determined by the sampling rate of 200 samples per second.

The short-period noise is the most variable. Figure 4-3 shows a 3-hour time window of unfiltered data from the vertical component of Temp-2 on 15 October 2013 from 00:20 to 03:00 UTC. The time history is at the top (Figure 4-3a), with the three spectrograms of the noise at different spectral bands below (Figures 4-3b through d). Prominent features in the spectrogram include a continuous hum with a frequency of about 82.7 Hz that dissipates after about 1.5 hours (Figure 4-3c) and bands of noise waxing and waning between 10 and 30 Hz (Figures 4-3b and d). Guralp observed these noise features in several data samples. In the absence of known seismic sources with these characteristics, Guralp interpreted these features as sound waves from distant sources causing vibration of the instruments directly or through coupling with the seafloor. In addition, the cool blue and light green colors of the high-frequency spectrogram suggest that although the short-period noise dominates the spectrogram, it is not the most intense.

Figure 4-4 shows long-period noise samples over 3 hours, from 15:00 to 18:00, on 8 August 2013 for horizontal components of Temp-1 and Temp-2. In contrast to the short-period noise sample, the long-period noise sample for the temporary units is not nearly as variable. While the diffuse band of yellow and red colors indicates prominent noise energy between 0.4 and 0.5 Hz (2.5 to 2 second [s] period), the dominant band (deep red) has an even lower frequency of below 0.1 Hz (10 s period).

Figure 4-5a is a noise sample of the DPG taken on the same day as the long-period sample of Temp-1 and Temp-2 on Figure 4-4. The DPG data are recorded for a longer period of time, from 06:00 to 23:00, which includes the 15:00 to 18:00 time period for Figure 4-4. Similar to Figure 4-4, there is a band of diffuse energy in the spectrogram of the DPG shown on Figure 4-5a around a 2 s period and the dominant energy band (purple color) is at the bottom at about a 14 s period. The DPG records changes of water pressure acting on the OBS. The main cause for these changes in the shallow depth at which all instruments of this OBS network are deployed is changes in the hydrostatic pressure due to ocean waves traveling over the deployment area. Guralp's interpretation is that the diffuse band at about 2 s represents waves driven by local winds, while the more intense band at 14 s is caused by the longer-period ocean swell generated by distant storms.

Figure 4-5b is an energy density spectrum of the ocean waves from the waverider buoy also on 8 August 2013 at about 16:00 UTC. The waverider buoy is a Datawell MkIII directional buoy operated by PG&E, located in water 22 m deep between OBS-4 and the DCP.P intake (Figure 4-1). The waverider buoy data show a dominant wave period of 14 s and a lesser energy but broader wave period at 5 s, consistent with what is observed in the seismic (Figure 4-4) and DPG data (Figure 4-5a). However, the waverider buoy does not show a peak at 2 s.

The noise described on Figures 4-3 through 4-5 can be seen with various intensities on both temporary units daily and simultaneously, indicating that the source is not in the immediate area. Guralp observed other noise recordings that could be seen on only one of the units. An example is shown on Figure 4-6. The three traces for Temp-1 and Temp-2 show general background noise for approximately the first 20 s. At approximately 17:50, Temp-2 abruptly starts showing high-amplitude, short-duration peaks and troughs, while Temp-1 remains relatively quiet. Guralp concluded that the abrupt change in pattern of Temp-2 was probably caused by marine animals bumping the units or climbing over them. The ROV crew assisting Guralp during the recovery of the portable OBS reported numerous animal sightings, among them a large sea star crawling over the instruments.

4.2 Analysis of Earthquakes Recorded by the OBS Units

In the Shoreline Fault Zone Report, hypocentral uncertainties for earthquakes that comprise the Shoreline seismicity lineament were estimated to be ± 0.5 km horizontal and ± 1 km vertical, based on two independent analyses of Hardebeck's double-difference location results (Appendix C to PG&E, 2011). A goal is to record data from the OBS stations to improve the azimuthal coverage, and thus improve the location results and focal mechanisms in the offshore DCP.P region, particularly in the region where the Shoreline fault approaches the Hosgri fault zone.

In this section we analyze four small ($<M 2.5$) earthquakes that occurred in the DCP.P region after 24 November 2013, when the OBS units were all in operation. The earthquakes are numbered 1 through 4, starting with the oldest event, and are listed in Table 4-1.

Events 1, 2, and 4 occurred in the region offshore from the DCP.P, with Events 1 and 4 along the Hosgri fault zone, and Event 2 northeast of the Hosgri fault zone; Event 3

occurred onshore in the Irish Hills approximately 8 km north of the DCP.P. The USGS earthquake locations and waveforms from each station are sent to the Northern California Earthquake Data Center at the University of California, Berkeley, where the magnitudes for each event are computed. The final location data, including the magnitudes are added to the Northern California Seismic Network (NCSN) catalog. The original, or starting, locations in the analysis described in Section 4.2.1 are in the NCSN catalog. Even though none of the offshore events are located between the OBS and onshore stations, we had the opportunity to study the effect of the additional offshore station coverage of nearby onshore and offshore earthquakes

4.2.1 Analytical Tests

For our analysis we conducted up to three tests on the data for each earthquake, computing new locations using HYPOINVERSE-2000 and focal mechanisms using FPFIT (Reasenber and Oppenheimer, 1985), and then comparing the results to the original NCSN catalog locations and focal mechanisms. Focal mechanisms represent fault plane solutions that best fit a given set of observed first-motion polarities for an earthquake. FPFIT may compute multiple solutions, which means that each solution fits the data equally.

For each event, the original catalog phase data included OBS time picks for at least OBS-4. Figure 4-7 shows the locations of the original catalog; the results of the three tests are described below and presented in Table 4-1. The original catalog location and the three tests are color coded on Figure 4-7 and Table 4-1 to aid in tracking the results.

- **Original catalog (green).** Shows the original earthquake locations as reported in the NCSN catalog.
- **Test 1 (red).** Relocates the earthquakes using the NCSN catalog phase data with the PG&E velocity model and recalculates the focal mechanism. The PG&E and USGS velocity models are compared on Figure 4-8. The USGS model is for the south-central California coast (Oppenheimer et al., 1993). The models are quite similar; however, except for the depth range centered at about 5 km, the USGS model is faster than the PG&E model.
- **Test 2 (yellow).** Relocates the earthquakes using the PG&E velocity model after taking out the OBS P- and S-wave readings, and recalculates the location.
- **Test 3 (purple).** Relocates the earthquakes depending on two sets of criteria: (1) if the original catalog did not include all available OBS P- and S-wave arrival times and P-wave first motions or (2) if the original catalog data did not include S-wave picks from the OBS units. Adds the new data and reruns the analysis using the USGS velocity model. Recalculates the focal mechanisms. Note that Event 1 met the first criteria and Event 3 met the second criteria.

4.2.2 Earthquake Relocation Results

The waveforms recorded on the broadband seismometers are shown for each of the four events on Figures 4-9, 4-14, 4-18, and 4-23, respectively. The OBS-2 and OBS-4

recordings look very good, and this is particularly positive for OBS-4 because it sits the closest to rocky substrate. OBS-1 shows ringing throughout the seismogram on all three events it recorded. OBS-3 shows similar ringing on two of the three events it recorded, but the ringing is only visible in the P-wave phases at the beginning of the event. The ringing suggests that OBS-1 and OBS-3 may not have established good coupling to the seafloor. We have been told by Guralp that it can take several months for the instruments to settle flat on the seafloor.

Figure 4-7 shows that the largest differences between the offshore relocations are generally less than a kilometer. Except for Event 2, the relocations group according to the velocity model used by HYPOINVERSE-2000. For example, the Event 1 test locations using the PG&E model (red circles = with OBS, and yellow circles = no OBS) are nearly the same, as are the locations using the USGS model (green circles = original, and purple circles). This indicates that the choice of velocity model is the dominant factor. This also indicates that for these earthquakes the velocity model has more effect on the locations than the presence of the OBS units. Interestingly, the root mean square values for the original and test runs that were used to invert for the calculated travel times and that are controlled by the velocity model do not vary significantly within each event.

The depth control for all four events is generally good, primarily because the closest station to the epicenter is equal to or less than the focal depth of the earthquakes. The exceptions are the three offshore events when no OBS units are used (yellow tests). In comparing the red test to the yellow test, where both tests use the same PG&E model, the depths are computed deeper when the OBS units are not used in the location (Table 4-1). The exception is Event 2, the 8 February 2014 earthquake east of the Hosgri fault zone, a very small event that appears to be more controlled than the other events by the OBS picks, as shown by the substantial increase in the azimuthal gap when the OBS units are removed.

4.2.3 Earthquake Focal Mechanism Results

The focal mechanisms for the original catalog locations and test results for each of the four events are shown on Figures 4-10 through 4-13, 4-15 through 4-17, 4-19 through 4-22, and 4-24 through 4-26, respectively. Except for Event 1/Test 2 (Figure 4-12) and Event 3/Test 1 (Figure 4-20), the original locations and the test results from FPFIT produced multiple solutions. Multiple solutions occur when more than one solution equally fits the input first-motion data. Multiples indicate that additional information may be needed to choose a preferred mechanism, such as knowledge about nearby faults (e.g., strike-slip or reverse motion) or regional tectonics (e.g., transpression or transtension environment).

Focal mechanisms are highly uncertain for events outside a network, even though the OBS data provided closer stations and improved depth control for the offshore events. The tests produced different mechanisms for the three offshore events. Event 1, the largest event in the analysis, has many first motions, yet very different mechanisms were produced by the FPFIT program when the number of OBS first motions went from one to all four OBS units. The most stable focal mechanisms are for Event 3, the M 1.24

earthquake in the Irish Hills. All but Test 1 (red) produced multiple solutions; however, each test, including Test 2 (yellow), with no OBS first motion used, produced a consistent northwest-trending reverse fault as the primary mechanism. This is not surprising as this event is well recorded with a very low azimuthal gap (Table 4-1). Event 4, another very small earthquake (M 0.88), has OBS-4 with a good S-wave pick; however, the focal mechanisms from each test are very different, which suggests unstable mechanisms. The results of the tests for each event are summarized in Table 4-2.

The results show that the only event with fairly stable (repeatable) focal mechanisms is Event 3, the onshore M 1.24 earthquake on 11 February 2014. This event has good station coverage (i.e., low azimuthal gap between stations), and at least one station is close by, within a focal depth distance from the epicenter. The other three events are offshore and outside the network, including the OBS stations. However, this study has shown that running tests such as these can produce consistent mechanisms that may have geologic significance. The results from removing the OBS first motions (Test 2) are equivocal primarily because these events are outside the network.

Table 4-1. Analysis of Earthquakes Recorded by OBS

Event No. (Date/ Magnitude)	Test (Color Code per Fig. 4-7)	Test	Time (UTC)	Latitude (deg.)	Longitude (deg.)	Depth (km)	Closest Station (km)	Azimuthal Gap (deg.)	No. of First Motions
1 (28 Nov. 2013/ M 2.35)	Original location (Green)	Original NCSN Catalog Data with OBS-4 Data (USGS Velocity Model)	14:29:10.23	35.1682	-120.9052	3.05	4	194	74
	Test 1 (Red)	Original NCSN Catalog Data with OBS-4 Data (PG&E Velocity Model)	14:29:10.07	35 10.35	-120 54.38	3.89	7	192	74
	Test 2 (Yellow)	Original NCSN Catalog Data with No OBS Data (PG&E Velocity Model)	14:29:10.11	35 10.38	-120 54.32	4.82	7	192	73
	Test 3 (Purple)	Original NCSN Catalog Data with All OBS Data (USGS Velocity Model)	14:29:10.25	35 10.01	-120 54.31	3.4	4	194	65
2 (8 Feb. 2014/ M 0.81)	Original location (Green)	Original NCSN Catalog Data with OBS-1 and -4 Data (USGS Velocity Model)	03:06:58.15	35.3055	-120.9452	9.01	4	142	21
	Test 1 (Red)	Original NCSN Catalog Data with OBS-1 and -4 Data, (PG&E Velocity Model)	03:06:57.97	35 18.62	-120 56.84	8.66	4	138	21
	Test 2 Yellow	Original NCSN Catalog Data with No OBS Data (PG&E Velocity Model)	03:06:57.90	35 18.32	-120 56.44	7.8	7	191	19

Table 4.1 (continued)

Event No. (Date/ Magnitude)	Test (Color Code per Fig. 4-7)	Test	Time (UTC)	Latitude (deg.)	Longitude (deg.)	Depth (km)	Closest Station (km)	Azimuthal Gap (deg.)	No. of First Motions
3 (11 Feb. 2014/ M 1.24)	Original location (Green)	Original NCSN Catalog Data with All OBS Data (USGS Velocity Model)	13:51:37.10	35.2727	-120.8347	7.34	3	55	24
	Test 1 (Red)	Original NCSN Catalog Data with All OBS Data (PG&E Velocity Model)	13:51:36.92	35 16.63	-120 50.06	7.97	2	57	24
	Test 2 Yellow	Original NCSN Catalog Data with No OBS Data (PG&E Velocity Model)	13:51:36.89	35 16.63	-120 50.26	8.06	2	75	20
	Test 3 Purple	Original NCSN Catalog Data with All OBS Data and added PG&E S-Wave Picks, (USGS Velocity Model)	13:51:37.10	35 16.39	-120 50.19	7.9	3	54	25
4 (1 Apr. 2014/ M 0.88)	Original location (Green)	Original NCSN Catalog Data with OBS-4 Data (USGS Velocity Model)	08:52:17.81	35.1432	-120.8727	4.04	5	199	14
	Test 1 (Red)	Original NCSN Catalog Data with OBS-4 Data, (PG&E Velocity Model)	08:52:17.72	35 08.83	-120 52.10	3.87	5	198	14
	Test 2 Yellow	Focal Mechanisms for the M 0.88 Earthquake on 01 Apr 2014— Original NCSN Catalog Data with No OBS Data (PG&E Velocity Model)	08:52:17.72	35 08.78	-120 52.14	4.09	8	199	13

Table 4-2. Results of Event Tests

Event	Test 1 (PG&E Velocity Model)	Test 2 (No OBS First Motions Used)	Test 3 (Different Criteria)
<p>Event 1 One OBS first motion (OBS-4) <i>Total: 74 first motions</i></p>	<p>(See Fig. 4-11)</p> <ul style="list-style-type: none"> Compared to the original catalog locations (Fig. 4-10), although both depths are shallow, the location using PG&E model is approximately 1 km deeper at 3.9 km. This does not seem to affect the focal mechanisms, however. Top and bottom solutions are quite similar (Fig. 4-10a vs. Fig. 4-11a; Fig. 4-10b vs. Fig. 4-11b). The mechanism is quite different from the singular mechanism without OBS (Fig. 4-12). The Test 1 multiple (Fig. 4-11b) is similar to the top mechanism (Fig. 4-13a) with all the OBS first motions. 	<p>(See Fig. 4-12)</p> <ul style="list-style-type: none"> Very different singular focal mechanism from the other results. Could be considered higher quality because only one mechanism fits the data given this criterion. 	<p><i>With OBS-2, -3, and -4 first motions and S-wave arrival times added:</i></p> <p>(See Fig. 4-13)</p> <ul style="list-style-type: none"> The top focal mechanism from Test 3 (Fig. 4-13a) is similar to the bottom mechanisms for Test 1 (Fig. 4-11b) and the original catalog location (Fig. 4-10b). These similar mechanisms may represent a stable solution for this event.
<p>Event 2 Two OBS first motions (OBS-1 and OBS-4) <i>Total: 21 first motions</i></p>	<p>(See Fig. 4-16)</p> <ul style="list-style-type: none"> The top mechanism (Fig. 4-16a) is similar to the other top mechanisms, regardless of whether the velocity model is changed (Fig. 4-15a) or the OBS first motions are removed (Fig. 4-17a). However, the bottom mechanism of Test 1 (Fig. 4-16b) is practically opposite of the bottom mechanisms of the original location (Fig. 4-15b) and Test 2 with no OBS first motions (Fig. 4-17b). The relative stability of the top mechanisms suggests that they may represent the actual fault motion. 	<p>(See Fig. 4-17)</p> <ul style="list-style-type: none"> The top and bottom mechanisms (Fig. 4-17a and 4-17b) are similar to the original mechanisms (Fig. 4-15a and 4-15b) and to the top mechanism of Test 1 (Fig. 4-16a). 	<p>[No new picks were added.]</p>

Table 4.1 (continued)

Event	Test 1 (PG&E Velocity Model)	Test 2 (No OBS First Motions Used)	Test 3 (Different Criteria)
<p>Event 3 All four OBS first motions <i>Total: 24 first motions</i></p>	<p>(See Fig. 4-20)</p> <ul style="list-style-type: none"> • This singular mechanism is quite similar to the top mechanism of the original location (Fig. 4-19a), the top mechanism of Test 2 showing no OBS readings (Fig. 4-21a) and the top mechanism of Test 3 with added S wave (Fig. 4-22a). • The singular solution produced by FPFIT suggests that the PG&E velocity model works best in this onshore region. 	<p>(See Fig. 4-21)</p> <ul style="list-style-type: none"> • Removing all four OBS first motions does not change the top mechanism (Fig. 4-21a) from the other top mechanisms (Figs. 4-19a and 4-22a) or the singular mechanism in Fig. 4-20. • The bottom mechanism of Test 2 (Fig. 4-21b) is considerably different from the original catalog multiple (Fig. 4-19b) and the multiple from Test 4 where S-wave data are added (Fig. 4-22b). • The similar northwest-trending reverse mechanism for the original and all tests suggests this is the likely mechanism for this earthquake. • The presence or absence of OBS generally does not affect the mechanism. 	<p><i>With S-wave arrival times added for all OBS:</i> (See Fig. 4-22)</p> <ul style="list-style-type: none"> • Both top and bottom mechanisms from this test (Fig. 4-22a and 4-22b) are quite similar to the top and bottom mechanisms in the original catalog data (Fig. 4-24a and 4-24b). The similarity is not surprising because the only difference in this test is the addition of two S-wave readings that are a little more than focal depth distance away from the event. (Only OBS-1 and OBS-4 were actually used in the location; OBS-2 and OBS-3 had weights too low to be used in the solution.)
<p>Event 4 One OBS first motion (OBS-4) <i>Total: 14 first motions</i></p>	<p>(See Fig. 4-25)</p> <ul style="list-style-type: none"> • Multiple solutions of Fig. 4-25 are very different from the original location multiples (Fig. 4-24a and 4-24b). • Mechanisms show little similarity among the test results. • This is an unstable, small (M 0.88) event; few first motions, including only 4 impulsive first motions, and poor depth control. 	<p>(See Fig. 4-26)</p> <ul style="list-style-type: none"> • The top mechanism from this test (Fig. 4-26a) is quite different from any of the other focal mechanisms computed for this event, but the bottom mechanism from this test (Fig. 4-26b) is similar to the top mechanism of the original catalog location (Fig. 4-25a). 	<p>[No new picks were added.]</p>

5.0 SOFTWARE

For the earthquake analyses in Section 4.2, HYPOINVERSE-2000 (Klein, 2002) was used to relocate the earthquakes, and FPFIT (Reasenber and Oppenheimer, 1985) was used to calculate focal mechanisms. Both programs are USGS open-source programs and are available free to the public from the USGS. The programs were tested, peer reviewed, and documented in the corresponding references.

6.0 CONCLUSIONS

The Point Buchon OBS Project succeeded in installing a four-OBS cabled system and transmitting the data to a data-receiving station onshore, and ultimately integrating with data from the NCSN recordings for the USGS's earthquake monitoring. The noise survey recorded on the temporary units provided an excellent look at the noise sources in this shallow environment, and provided confirmation that the DPG worked properly because it recorded the same noise information as the temporary units.

The analysis of four small earthquakes recorded on the long-term units reaffirmed that offshore events close to but outside the OBS stations will have improved depth control; however, these events are still subject to uncertainty, particularly with regard to the focal mechanisms.

The project activities met with several challenges, such as the involved process of obtaining a lease and permits from state and federal agencies and the restrictions on our proposed scientific methods. In addition, deploying the cabled system in shallow waters (<120 m) required focused tactics due to variable tides, currents, weather, and marine life. Nevertheless, our initial results show that the OBS system is capable of recording earthquakes of magnitude just above 1 at distances of about 10 km.

7.0 REFERENCES

California State Lands Commission (CSLC), 2012. *Mitigated Negative Declaration for the Pacific Gas and Electric (PG&E) Point Buchon Ocean Bottom Seismometer Project*, State Clearinghouse (SCH) No. 2011081079, March.

Hardebeck, J.L., 2010. Seismotectonics and fault structure of Central California, *Bulletin of the Seismological Society of America* **100** (3): 1031–1050.

Hardebeck, J.L., 2013. Geometry and earthquake potential of the Shoreline fault, central California, *Bulletin of the Seismological Society of America* **103** (1): 447–462.

Hardebeck, J.L., and Shearer, P.M., 2002. A new method for determining first-motion focal mechanisms, *Bulletin of the Seismological Society of America* **92**: 2,264–2,276.

Klein, F.W., 2002. *User's Guide to HYPOINVERSE-2000, a Fortran Program to Solve for Earthquake Locations and Magnitudes*, U.S. Geological Survey Open-File Report 02-171, 4/2002 program version, 122 pp.

McLaren, M.K., and Savage, W.U., 2001. Seismicity of south-central coastal California: October 1987 through January 1997, *Bulletin of the Seismological Society of America* **91** (4): 1629–1658.

Oppenheimer, D., Klein, F., Eaton, J., and Lester, F., 1993. *The Northern California Seismic Network Bulletin: January–February 1992*, U.S. Geological Survey Open-File Report 93-578, 48 pp.

Ouillon, G., Ducorbier, C., and Sornette, D., 2008. Automatic reconstruction of fault networks from seismicity catalogs: Three-dimensional optimal anisotropic dynamic clustering, *Journal of Geophysical Research: Solid Earth* **113** (B1), doi:10.1029/2007JB005032.

Pacific Gas and Electric Company (PG&E), 2011. *Shoreline Fault Zone Report: Report on the Analysis of the Shoreline Fault Zone, Central Coastal California*, report to the U.S. Nuclear Regulatory Commission, January; www.pge.com/myhome/edusafety/systemworks/dcpp/shorelinereport/.

Reasenber, P., and Oppenheimer, D., 1985. *FPPFIT, FPPLLOT and FPPAGE: Fortran Computer Programs for Calculating and Displaying Earthquake Fault-Plane Solutions*, U.S. Geological Survey Open-File Report 85-739, 109 pp.

Waldhauser, F., 2001. *HypoDD: A Computer Program to Compute Double-Difference Hypocenter Locations*, U.S. Geological Survey Open-File Report 01-113, 25 pp.

Zhang, H., and Thurber, C.H., 2003. Double-difference tomography: The method and its application to the Hayward Fault, California, *Bulletin of the Seismological Society of America* **93**: 1875–1889.

ATTACHMENT 1

REPORT VERIFICATION SUMMARY

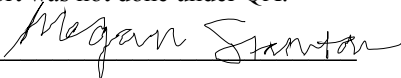
An Independent Technical Reviewer (ITR) provided reviews of the Technical Report and supporting documents. Megan Stanton reviewed the report for technical accuracy, including use of proper interpretation methods and for compliance with PG&E Geosciences report standards and formats.

Report Verification Summary by Independent Technical Reviewer

Item	Parameter	Yes	No*	N/A*
1	Purpose is clearly stated and the report satisfies the Purpose.	Y		
2	Data to be interpreted and/or analyzed are included or referenced.	Y		
3	Methodology is appropriate and properly applied.	Y		
4	Assumptions are reasonable, adequately described, and based upon sound geotechnical principles and practices.	Y		
5	Software is identified and properly applied. Validation is referenced or included, and is acceptable. Input files are correct and accurate.	Y		
6	Interpretation and/or Analysis is complete, accurate, and leads logically to Results and Conclusions.	Y		
7	Results and Conclusions are accurate, acceptable, and reasonable compared to the Data, interpretation and/or analysis, and Assumptions.	Y		
8	The Limitation on the use of the Results has been addressed and is accurate and complete.			N/A
9	The Impact Evaluation has been included and is accurate and complete.			N/A
10	References are valid for intended use.	Y		
11	Appendices are complete, accurate, and support the text.	Y		

* Explain "No" or "N/A" entries. (For example, Items 3 thru 7 would be N/A for a data report that simply presents the collected data.)

Items 8 and 9 are N/A because this report was not done under QA.

Verifier (ITR): Megan Stanton  06/26/14
 (name/signature) (date)